Bias Sputtered NbN and Superconducting Nanowire Devices

Andrew E. Dane[1], Adam N. McCaughan[1,2], Di Zhu[1], Qingyuan Zhao[1], Chung-Soo Kim[1], Niccolo Calandri[1,3], Akshay Agarwal[1], Francesco Bellei[1], Karl K. Berggren[1]

[1]Department of Electrical Engineering and Computer Science, Massachusetts Institute of Technology, 77 Massachusetts Avenue, Cambridge, Massachusetts 02139, USA

[2]National Institute of Standards and Technology, 325 Broadway, Boulder, Colorado 80305, USA

[3]Dipartimento di Elettronica, Informazione e Bioingegneria, Piazza Leonardo da Vinci 32, 20133 Milano, Italy

Superconducting nanowire single photon detectors (SNSPDs) promise to combine near-unity quantum efficiency with >100 megacounts per second rates, picosecond timing jitter, and sensitivity ranging from x-ray to mid-infrared wavelengths. However, this promise is not yet fulfilled, as superior performance in all metrics has yet to be combined into one device. The highest single-pixel detection efficiency and the widest bias windows for saturated quantum efficiency have occurred in SNSPDs based on amorphous materials, while the lowest timing jitter and highest counting rates were demonstrated in devices made from polycrystalline materials. Broadly speaking, the amorphous superconductors that have been used to make SNSPDs have higher resistivities and lower T_c values than typical polycrystalline materials. Here we demonstrate a method of preparing niobium nitride (NbN) that has lower-than-typical superconducting transition temperature, and higher-than-typical resistivity. As we will show, NbN deposited onto unheated SiO_2 has a low T_c and high resistivity, but is too rough for fabricating unconstricted nanowires, and the T_c is too low to yield SNSPDs that can operate well at liquid helium temperatures. By adding a 50 W RF bias to the substrate holder during sputtering, the T_c of the unheated NbN films was increased by up to 73%, and the roughness was substantially reduced. After optimizing the deposition for nitrogen flow rates, we obtained 5nm thick NbN films with a T_c of 7.8 K and a resistivity of 253 μΩcm. We used this bias sputtered room temperature NbN to fabricate SNSPDs. Measurements were performed at 2.5K using 1550nm light. Photon count rates appeared to saturate at bias currents approaching the critical current, indicating that the device's quantum efficiency was approaching unity. We measured a single-ended

timing jitter of 38 ps. The optical coupling to these devices was not optimized; however, integration with front-side optical structures to improve absorption should be straightforward. This material preparation was further used to fabricate nanocryotrons as well as a large-area imager device, reported elsewhere. The simplicity of the preparation and promising device performance should enable future high-performance devices.

Introduction and background:

For a variety of emerging quantum- and nano-devices, performance is limited by material synthesis and device fabrication. These limitations are especially evident in sensitive photon detectors [1] and quantum computing elements [2]. The superconducting nanowire single photon detector (SNSPD) [3] promises to combine near 100% detection efficiency [4] with >100 megacounts per second, picosecond timing jitter [5], and sensitivity ranging from x-rays to mid-infrared wavelengths [6]. However, this promise is not yet fulfilled, as superior performance in all metrics has yet to be combined into one device. The link between SNSPD performance and material properties is still being studied [7]. The addition of amorphous superconductors to the palette of demonstrated SNSPD materials has advanced the state of the art. The short time between the introduction of WSi [8] and the leap in maximum demonstrated single-pixel system detection efficiency [9] indicates that substantial opportunity exists for improving SNSPDs by engineering the materials used to make them.

The central problem that we hope to address through tailoring superconducting niobium nitride (NbN) for SNSPDs is that the highest single-pixel detection efficiency and deepest saturation have occurred in SNSPDs based on amorphous materials [4], while the lowest timing jitter and highest counting rates were demonstrated in devices made from polycrystalline materials [5]. Our goal was to combine the detection efficiency performance of the amorphous detectors with the timing performance and operating temperature of the polycrystalline ones. We employed an empirical approach to making a material suitable for this task because, despite gains in our understanding about how SNSPDs work [10][11], a full description of the detector operation is still being developed [12]. Whether it is possible to combine the best properties of these two materials systems into one device or whether there exists an intrinsic trade-off between the detection and timing performance remains to be seen.

The superconducting and normal-state properties of NbN films are affected by the stochiometry [13], crystal phase [14], impurity content [15], disorder [16], thickness [17], and carrier concentration [18], all of which can be influenced by the deposition method. Ultrathin NbN films are commonly prepared by reactive sputtering of a niobium target in a mixture of argon and nitrogen (N_2) gas. Amorphous substrates have been used when depositing sputtered films; however, films prepared on crystalline substrates suitable for epitaxy show higher superconducting critical temperature (T_c), and lower resistivity at the same thicknesses [19]. Intentional heating of the substrate to temperatures of a few-hundred degrees Celsius or more has been used to improve the crystalline properties of the deposited film, though ambient temperatures combined with lattice-matched substrates have demonstrated 5-nm-thick films, a thickness relevant for SNSPDs, with 12 K T_c [13].

In this work, we show that the addition of ion bombardment during the sputter deposition of ultrathin NbN films onto unheated, thermally-oxidized silicon can increase film T_c and reduce film resistivity and that the resulting material can be fabricated into SNSPDs with saturated internal efficiency and 38 ps jitter at a temperature of 2.5 K. Following the suggestion that a reduced superconducting energy gap may lead to improved detection efficiency [20], we modified the typical sputter deposition method used to make ultrathin films of NbN to reduce the film T_c. By removing the usual substrate heating to ~800 °C, the NbN film T_c and maximum grain size (see supplementary materials) were both reduced. However, 5-nm-thick films deposited at ambient temperature have critical temperatures that we believe are too small to yield devices with ~10 ps jitter while operating at liquid helium temperatures, and thicker unheated NbN films have substantial surface roughness which would likely lead to constrictions [10]. Both of these issues were addressed by the addition of ion bombardment due to substrate biasing during deposition. Using bias sputtered NbN films, we demonstrated SNSPDs and nanocryotrons (nTrons) [21]. This material was also used to fabricate a large-area single photon imager, reported elsewhere [22].

Experiment and Results:

The experimental work of this letter can be divided into three parts: (1) the characterization of NbN sputter deposition rates under different chamber conditions, (2) the deposition and electrical characterization of 5-nm-thick NbN films, and (3) fabrication and testing of SNSPDs and nTrons based on films prepared in step two. To compare 5-nm-thick thick films deposited under different chamber conditions, changes to the film deposition rate had to be measured and then compensated for. Relatively thick films (~20-30 nm) were deposited, and their thicknesses were measured using x-ray reflectivity (XRR) to determine the deposition rate for each of the conditions studied. At each chamber condition, the sputtering time was subsequently adjusted to yield 5-nm-thick films. Electrical characterization of the thin films included four-point probe measurements of film T_c and sheet resistance. SNSPDs and nTrons were fabricated using optical and electron beam lithography. SNSPDs were measured with a 1550 nm photon input while at 2.5K.

All films discussed in this work were deposited in a dedicated AJA International Inc Orion series sputtering system by DC reactive magnetron sputtering from a sputter gun source, in a cryopumped chamber with a typical base pressure of 6.7×10^{-7} Pa (5×10^{-9} Torr). The DC current was set to 400 mA and the sputtering pressure was 3.3×10^{-1} Pa (2.5×10^{-3} Torr) for all depositions. The flow rate of Ar was 26.5 cm^3/min, while the N_2 flow was varied as shown. 14 W of RF power was applied to the 4-inch diameter sample holder from an external RF source and matching network in order to sputter-clean samples prior to deposition. For bias sputtered samples, the RF power was increased to 50 W during the deposition step of the process which caused a DC voltage of approximately -280V to develop at the sample holder. Otherwise, the sample bias was turned off during the sputtering step. No intentional heating, via heat lamps or heater elements, was added. Additional details are provided in the supplementary materials.

Altering the chamber conditions in order to tune the T_c of reactively sputtered NbN has the unwanted effect of changing the film deposition rate [23] and makes it more difficult to judge which films will make the best SNSPDs, because the film T_c is a strong function of thickness in the few-nanometer regime, approaching the superconductor-insulator transition [17]. Our initial attempts to deposit few-nanometer-thick NbN without heating resulted in films with T_c values of less than 5 K, less than half of what we observed while heating to 800 °C [24]. The relative amount of nitrogen and niobium in NbN films is a primary influence on the film T_c and resistivity [25][26]. Therefore, to increase the T_c of the films deposited at ambient temperature, we varied the relative ratio of nitrogen and niobium in the film by changing the nitrogen flow rate. Additionally, we found that by adding a 50 W RF bias to the substrate holder, we could almost double the observed T_c. Initially, it was unclear if this effect was due to changes in the film quality, or due to an increase in the deposition rate due to the RF bias increasing the plasma density, as observed in reference [27]. To determine the source of this effect, we characterized the deposition rate at the each of the chamber conditions in question.

Figure 1 details the effect of different chamber conditions, including changing N_2 flow rates and the addition of a 50W RF bias, on the deposition rate and properties of NbN. Cross-sectional transmission electron microscope (XTEM) images in Figure 1a show the structure and thickness of a film prepared with (top) and without (bottom) a 50 W RF bias applied during deposition. Less-than-100-nm-thick cross-sections were prepared using a gallium focused ion beam (FEI Helios Nanolab 600) and imaged in a field emission TEM (JEOL 2010F). While both films appear to be polycrystalline, the dark vertical stripes seen in the non-biased film are not evident in the film deposited with bias. The reduced surface roughness of the film prepared with bias is also evident. Figure 1b compares XRR measurements of the films imaged in (a). At incident angles greater than 2 degrees, interference fringes are more prominent for the film that was deposited with bias than without. Modeling and fitting the XRR curves using Rigaku's GlobalFit software reveal that the root-mean-squared (rms) film roughness was reduced from 1.7 nm to 0.8 nm due to the addition of the RF bias, while the film density increased from 7.2 g/cm^3 to 7.5 g/cm^3. Adding the bias during deposition reduced roughness and increased density for all pairs of films measured. The roughness values derived from XRR are about three times larger than what was measured with an atomic force microscope (see SM for AFM images). Figure 1c shows the deposition rate characterized by XRR for ten different deposition conditions. These films were deposited for 8 minutes, and measured thicknesses ranged from 46 nm for a film deposited with 2 cm^3/min of N_2 flow without bias to 23 nm for a film deposited with 10 cm^3/min of N_2 flow and a 50 W bias. On average, the addition of the bias reduced the film deposition rate by 12.8%. Top down TEMs of NbN prepared on SiO_2 TEM windows (see supplementary materials) show that the NbN films prepared for this work were polycrystalline, regardless of preparation method.

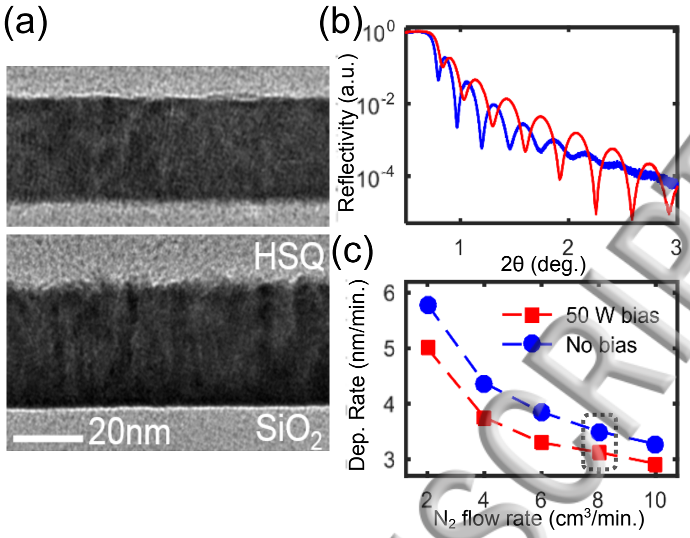

Figure 1. (a) Cross-sectional transmission electron microscope (XTEM) images of reactive DC magnetron sputtered niobium nitride (NbN) with (top) and without (bottom) a 50 W RF bias applied to the sample holder during the deposition. The texture of the two films is noticeably different, with the addition of the bias reducing or eliminating columnar grains [28] present in the film deposited without bias. XRD and top down TEM images (see supplementary materials) both indicate that the films are polycrystalline. (b) Experimental x-ray reflectivity (XRR) as a function of twice the incident angle for films shown in (a). Modeling of the measured interference pattern allows us to extract the NbN film density, thickness, and roughness. Film thickness estimated from TEM images matched the values derived from XRR to within 2 nm. (c) The deposition rate, as determined by XRR, for NbN films deposited for 8 min onto SiO_2 substrates at different flow rates of N_2, with and without bias, all else held constant. The addition of the bias reduced the measured deposition rate at a given N_2 flow, presumably due to resputtering of the deposited film. The points indicated are deposition rates estimated from the XRR measurements shown in (b) of the films imaged in (a). Repeated XRR thickness measurements of a given film varied by less than 0.1 nm.

After characterizing the deposition rate for different deposition conditions as shown in Figure 1c, we then deposited 5-nm-thick films by adjusting the deposition time. While the voltage drop across the plasma varied within the first one or two seconds after opening the shutter to begin the deposition, this transient period was much shorter than the shortest deposition time of 52 s. Therefore, we believe that we are in a regime where the thickness is well approximated by the product of the deposition rate and time. After the conclusion of all of the depositions for this work, we repeated the deposition of the very first film considered and measured its thickness with XRR. We found that the deposition rate had fallen by 3.6%. This reduction of deposition rate over time can be explained by a reduction in the voltage that develops between the plasma and the target, due to an effective increase in the magnetron trap strength as the sputter target is thinned [29][30].

In Figure 2, we show that the addition of a 50 W RF bias decreased the resistivity and increased the superconducting transition temperature for all of the 5-nm-thick films relative to comparable films prepared without bias. As shown in Figure 2a, the addition of the bias reduced the resistivity of the 5-nm-thick films by between 23% and 42%. For the 5-nm-thick films, the addition of the 50 W RF bias during deposition increased the film T_c by between 25% and 73%. The maximum T_c of the bias-sputtered 5-nm-thick films is close to what we believe is optimal for high detection efficiency, low jitter SNSPDs. The relative increase in T_c was nearly linear as a function of the N_2 flow rate, suggesting that the nitrogen content of the film contributed to low T_c in the thin film limit, possibly by promoting structural disorder that is overcome by ion bombardment. The resistivity and T_c of the thick films used to calibrate the deposition rates were also measured. For these films, resistivity was lowered in all cases by between 55% and 36% (see SM). In contrast, the T_c of the thick films prepared with bias was not always higher than without. The maximum T_c for the thick films with bias was about 500 mK (5%) lower than the maximum T_c for thick films deposited without bias. These results corroborate previous reports on bias sputtering of NbN [27][31], and it is clear that only in the nanometer thickness limit relevant for SNSPDs does the addition of ion bombardment substantially improve the film T_c.

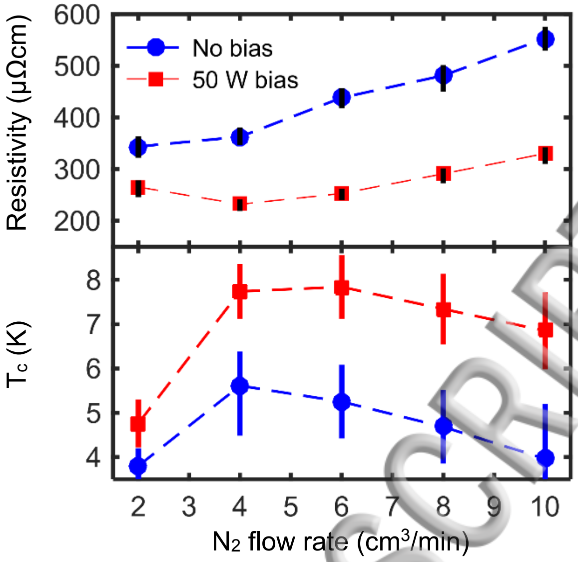

Figure 2. Room temperature resistivity (top) and superconducting critical temperature (bottom) for 5-nm-thick NbN films deposited with different chamber conditions. The deposition time at each N_2 flow rate and bias condition was adjusted so that the deposited film would be 5 nm thick. The addition of the bias reduced the room temperature resistivity and increased the T_c of a film deposited with identical conditions. Repeated measurements of film T_c gave the same value to within 30 mK, with a standard deviation of 13 mK. Resistivity was calculated from the sheet resistance measured by four point probe multiplied by the thickness (5 nm). Black error bars represent an upper-bound estimate of the error, based on a 3.6% growth rate reduction during the course of the entire experiment, combined with a ± 2 second error in deposition time and a ±1.5% error in the measured sheet resistance. The superconducting transition region is illustrated in the bottom graph by the colored bars which indicate the temperatures where the resistance was between 10% and 90% of its value at 20 K.

This material work was motivated by the desire to improve SNSPD performance, so after characterizing the bias sputtered films, we designed and fabricated 75 nm wide SNSPDs using 5-nm-thick NbN deposited with a 50 W RF bias and 6 cm^3/min N_2 flow onto oxidized silicon. The nanowires were fabricated in a standard meander pattern with the active area covering approximately 11 μm^2. Turnarounds were optimized to avoid current crowding and maximize the switching current of the device [32]. Gold electrical contact pads were fabricated on top of the NbN film by using photolithography. After gold pad fabrication, 10 nm of SiO_x was evaporated onto the surface of the NbN to protect it during subsequent fabrication steps and enhance adhesion of the electron-beam resist. Hydrogen silsesquioxane (HSQ; 6% concentration) was spin coated onto the chip at 3 krpm. The HSQ was exposed to a 125 keV electron beam with an areal dose density of 3,840 $\mu C/cm^2$. After exposure, the HSQ was developed by submerging the chip in 25% tetramethylammonium hydroxide for 25 s. The HSQ pattern was then transferred to the NbN by reactive ion etching in CF_4 at 50 W for 4 min.

Many of the promising applications for SNSPDs require picosecond timing resolution and the ability to detect single infrared photons in the telecommunications band. Therefore, we characterized the detection efficiency and timing jitter of the fabricated SNSPDs at 1550 nm wavelength. Figure 3 summarizes our results including saturated single photon detection efficiency at 1550 nm and timing jitter of 38 ps. SNSPD performance was characterized at 2.5 K, in vacuum, on the coldhead of a liquid helium flow cryostat, with measurement conditions identical to those previously reported [33]. The single-photon counting regime was confirmed by measuring the count rate from the SNSPD, which was linear as a function of the applied laser power. Figure 3a shows the counting rate of one of these devices as a function of the device bias current. The timing distribution with respect to the laser pulse was measured, yielding a jitter of 38 ps, full width at half maximum. By fitting to the exponential decay of a photoresponse voltage pulse, we estimated the kinetic inductance of the material to be approximately 150 pH per square. The large kinetic inductance of the bias sputtered material was used to advantage in a recently demonstrated nanowire imager device [22] and was also used to fabricate the recently introduced nTron [21], whose DC performance is shown in Figure 3d. While we did not attempt to maximize the coupling efficiency to our SNSPDs nor the maximum count rate, we believe that the saturated detection efficiency, combined with the 38 ps timing jitter, make this a promising material for combining high detection efficiency and low jitter in a single device that can operate at liquid helium temperatures.

In conclusion, we demonstrated that the addition of ion bombardment due to RF biasing of the substrate holder during the sputter deposition of few-nanometer-thick NbN films onto unheated SiO_2 substrates increased T_c and reduced resistivity, and we used this material to fabricate SNSPDs with saturated detection efficiency and 38 ps jitter. A nanowire imager [22] and nTrons were also demonstrated using the same material. While the addition of the bias decreased the film resistivity in all cases, the film T_c was not necessarily increased when deposited to tens of nanometers in thickness, indicating a decoupling of resistivity and critical temperature that could provide an experimental avenue for exploring a recently observed relation between thin film superconductor thickness, sheet resistance, and T_c [34]. This method of preparing NbN thin films at ambient temperatures should be compatible with a wider array of fabrication techniques and materials than NbN that is deposited at elevated temperatures or onto lattice matched substrates, and thus should enable fabrication processes that were previously not feasible. In particular, this method should allow easy integration of SNSPDs with existing photonic integrated circuits [35].

Supplementary Material:

See supplementary material for methods, T_c and resistivity data for thick NbN films, AFM, XPS and XRD data, as well as top down TEM images of different preparations of NbN.

Acknowledgments:

The authors would like to thank Jim Daley and Mark Mondol of the MIT Nanostructures lab for technical support related to electron beam fabrication. We would also like to thank Dr. Charles Settens from the

Center for Materials Science and Engineering X-ray Facility for his assistance and advice on all matters related to x-ray measurements. This work made use of the Shared Experimental Facilities supported in part by the MRSEC Program of the National Science Foundation under award number DMR - 1419807. Andrew Dane was supported by a NASA Space Technology Research fellowship, grant number NNX14AL48H. This research is based on work supported by the Office of the Director of National Intelligence (ODNI), Intelligence Advanced Research Projects Activity (IARPA), via contract W911NF-14-C0089. The views and conclusions contained herein are those of the authors and should not be interpreted as necessarily representing the official policies or endorsements, either expressed or implied, of the ODNI, IARPA, or the U.S. Government. The U.S. Government is authorized to reproduce and distribute reprints for Governmental purposes notwithstanding any copyright annotation thereon.

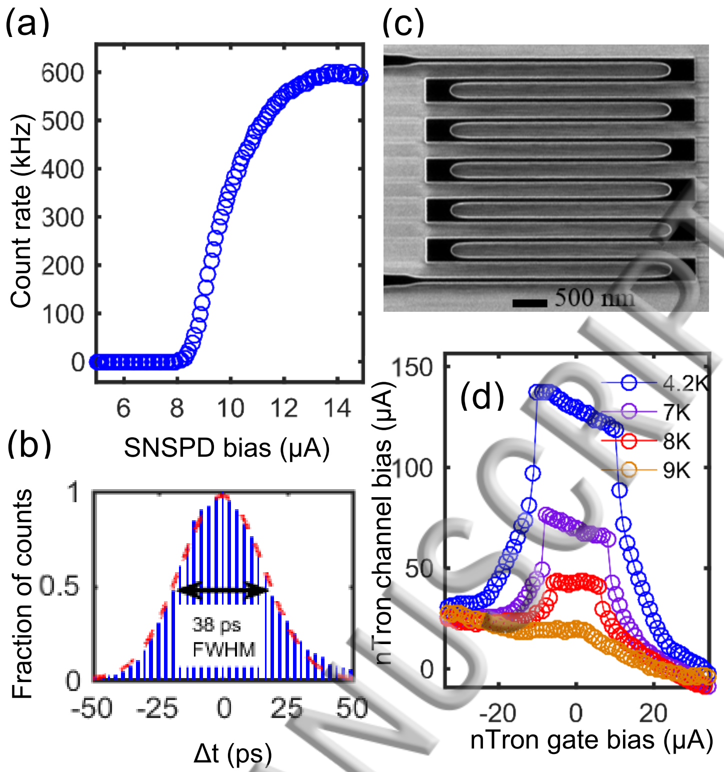

Figure 3. Measurements of devices made with bias sputtered NbN. (a) 1550 nm photon count rate of a 75 nm wide SNSPD fabricated from 5 nm thick bias-sputtered NbN as a function of bias current. The count rate appears to saturate, suggesting that the internal quantum efficiency of the SNSPD may be close to unity. The instrument response function is shown in (b), fit curve in red, with a full width at half maximum of 38 ps. (c) Helium ion microscope image of a representative SNSPD. (d) We also used bias sputtered NbN to fabricate the recently introduced nTron [21], whose DC transfer characteristic was measured at the 4 temperatures shown. The NbN was approximately 10 nm thick while the gate and channel widths were 30 nm and 400 nm, respectively.

[1] J. Gao, M. Daal, A. Vayonakis, S. Kumar, J. Zmuidzinas, B. Sadoulet, B. A. Mazin, P. K. Day, and H. G. Leduc, “Experimental evidence for a surface distribution of two-level systems in superconducting lithographed microwave resonators,” *Appl. Phys. Lett.*, vol. 92, no. 15, p. 152505, 2008.

[2] W. D. Oliver and P. B. Welander, “Materials in superconducting quantum bits,” *MRS Bull.*, vol. 38, no. 10, pp. 816–825, 2013.

[3] G. N. Gol’tsman, O. Okunev, G. Chulkova, a. Lipatov, a. Semenov, K. Smirnov, B. Voronov, a. Dzardanov, C. Williams, and R. Sobolewski, “Picosecond superconducting single-photon optical detector,” *Appl. Phys. Lett.*, vol. 79, no. 6, p. 705, 2001.

[4] F. Marsili, V. B. Verma, J. A. Stern, S. Harrington, A. E. Lita, T. Gerrits, I. Vayshenker, B. Baek, M. D. Shaw, R. P. Mirin, and S. W. Nam, “Detecting single infrared photons with 93 % system efficiency,” vol. 7, no. February, pp. 2–6, 2013.

[5] L. You, X. Yang, Y. He, W. Zhang, D. Liu, W. Zhang, L. Zhang, L. Zhang, X. Liu, S. Chen, Z. Wang, and X. Xie, “Jitter analysis of a superconducting nanowire single photon detector,” *AIP Adv.*, vol. 3, no. 7, p. 72135, 2013.

[6] F. Marsili, F. Bellei, F. Najafi, A. E. Dane, E. a. Dauler, R. J. Molnar, and K. K. Berggren, “Efficient single photon detection from 500 nm to 5 μm wavelength,” *Nano Lett.*, vol. 12, no. 9, pp. 4799–4804, 2012.

[7] D. Henrich, S. Dörner, M. Hofherr, K. Ilin, A. Semenov, E. Heintze, M. Scheffler, M. Dressel, and M. Siegel, “Broadening of hot-spot response spectrum of superconducting NbN nanowire single-photon detector with reduced nitrogen content,” *J. Appl. Phys.*, vol. 112, no. 7, 2012.

[8] B. Baek, A. E. Lita, V. Verma, and S. W. Nam, “Superconducting a-W[sub x]Si[sub 1−x] nanowire single-photon detector with saturated internal quantum efficiency from visible to 1850 nm,” *Appl. Phys. Lett.*, vol. 98, no. 25, p. 251105, 2011.

[9] F. Marsili, V. B. Verma, J. a. Stern, S. Harrington, a. E. Lita, T. Gerrits, I. Vayshenker, B. Baek, M. D. Shaw, R. P. Mirin, and S. W. Nam, “Detecting Single Infrared Photons with 93% System Efficiency,” *Nat. Photonics*, vol. 7, no. 3, pp. 210–214, Feb. 2013.

[10] A. J. Kerman, E. a. Dauler, J. K. W. Yang, K. M. Rosfjord, V. Anant, K. K. Berggren, G. N. Gol’tsman, and B. M. Voronov, “Constriction-limited detection efficiency of superconducting nanowire single-photon detectors,” *Appl. Phys. Lett.*, vol. 90, no. 10, p. 101110, 2007.

[11] A. J. Kerman, E. a. Dauler, W. E. Keicher, J. K. W. Yang, K. K. Berggren, G. Gol’tsman, and B. Voronov, “Kinetic-inductance-limited reset time of superconducting nanowire photon counters,” *Appl. Phys. Lett.*, vol. 88, no. 11, p. 111116, 2006.

[12] J. J. Renema, R. Gaudio, Q. Wang, Z. Zhou, a. Gaggero, F. Mattioli, R. Leoni, D. Sahin, M. J. a. de Dood, a. Fiore, and M. P. van Exter, “Experimental Test of Theories of the Detection Mechanism in a Nanowire Superconducting Single Photon Detector,” *Phys. Rev. Lett.*, vol. 112, no. 11, p. 117604, Mar. 2014.

[13] Z. Wang, A. Kawakami, Y. Uzawa, and B. Komiyama, “Superconducting properties and crystal structures of single-crystal niobium nitride thin films deposited at ambient substrate temperature,” *J. Appl. Phys.*, vol. 79, no. 10, p. 7837, 1996.

[14] G. Oya and Y. Onodera, “Transition temperatures and crystal structures of single-crystal and polycrystalline NbNx films,” *J. Appl. Phys.*, vol. 45, no. 3, pp. 1389–1397, 1974.

[15] M. J. Deen, “The Effect of The Deposition Rate on the Properties of DC-Magnetron-Sputtered Niobium Nitride Thin Films,” *Thin Solid Films*, vol. 152, pp. 535–544, 1987.

[16] V. Sadagopan, H. C. Gatos, K. Hechler, and E. Saur, “Fast neutron damage and the current carrying capacity of niobium nitride,” *Z Phys.*, vol. 225, no. 3, pp. 231–236, Jun. 1969.

[17] S. Ezaki, K. Makise, B. Shinozaki, T. Odo, T. Asano, H. Terai, T. Yamashita, S. Miki, and Z. Wang, “Localization and interaction effects in ultrathin epitaxial NbN superconducting films.,” *J. Phys. Condens. Matter*, vol. 24, no. 47, p. 475702, Nov. 2012.

[18] S. Chockalingam, M. Chand, J. Jesudasan, V. Tripathi, and P. Raychaudhuri, “Superconducting properties and Hall effect of epitaxial NbN thin films,” *Phys. Rev. B*, vol. 77, no. 21, p. 214503,

Jun. 2008.

[19] J. R. Gao, M. Hajenius, F. D. Tichelaar, T. M. Klapwijk, B. Voronov, E. Grishin, G. Gol'tsman, C. a. Zorman, and M. Mehregany, "Monocrystalline NbN nanofilms on a 3C-SiC/Si substrate," *Appl. Phys. Lett.*, vol. 91, no. 6, p. 62504, 2007.

[20] a. Engel, A. Aeschbacher, K. Inderbitzin, A. Schilling, K. Il'in, M. Hofherr, M. Siegel, A. Semenov, and H.-W. Hübers, "Tantalum nitride superconducting single-photon detectors with low cut-off energy," *Appl. Phys. Lett.*, vol. 100, no. 6, p. 62601, 2012.

[21] A. N. McCaughan and K. K. Berggren, "A Superconducting-Nanowire Three-Terminal Electrothermal Device.," *Nano Lett.*, vol. 14, pp. 5748–5753, Sep. 2014.

[22] Q.-Y. Zhao, D. Zhu, N. Calandri, A. E. Dane, A. N. McCaughan, F. Bellei, H.-Z. Wang, D. F. Santavicca, and K. K. Berggren, "Single-photon imager based on a superconducting nanowire delay line," *Nat. Photonics*, vol. 11, no. 4, pp. 247–251, 2017.

[23] S. Berg and T. Nyberg, "Fundamental understanding and modeling of reactive sputtering processes," *Thin Solid Films*, vol. 476, no. 2, pp. 215–230, Apr. 2005.

[24] F. Najafi, A. Dane, F. Bellei, Q. Zhao, K. A. Sunter, A. N. Mccaughan, K. K. Berggren, and S. Member, "Fabrication Process Yielding Saturated Nanowire Single-Photon Detectors With 24-ps Jitter," vol. 21, no. 2, 2015.

[25] H. Rogener, "Zur Supraleitung des Niobnitrids," *Zeitschrift fur Phys.*, vol. 132, pp. 446–467, 1952.

[26] a. V. Linde, R.-M. Marin-Ayral, F. Bosc-Rouessac, and V. V. Grachev, "Effect of nitrogen to niobium atomic ratio on superconducting transition temperature of δ-NbN x powders," *Int. J. Self-Propagating High-Temperature Synth.*, vol. 19, no. 1, pp. 9–16, Apr. 2010.

[27] W. L. Carter, E. J. Cukauskas, S. B. Qadri, a. S. Lewis, and R. J. Mattauch, "Effects of rf bias on the superconducting and structural properties of rf magnetron sputtered NbN," *J. Appl. Phys.*, vol. 59, no. 8, p. 2905, 1986.

[28] H. L. Ho, K. E. Gray, R. T. Kampwirth, D. W. Capone, and V. A, "Transverse transmission electron microscopy of sputtered NbN films," *J. Mater. Sci.*, vol. 21, pp. 4097–4100, 1986.

[29] D. Depla, K. Strijckmans, and R. De Gryse, "The role of the erosion groove during reactive sputter deposition," *Surf. Coatings Technol.*, vol. 258, pp. 1011–1015, Nov. 2014.

[30] D. Depla, S. Mahieu, and R. De Gryse, "Magnetron sputter deposition: Linking discharge voltage with target properties," *Thin Solid Films*, vol. 517, no. 9, pp. 2825–2839, Mar. 2009.

[31] Y. M. Shy, L. E. Toth, and R. Somasundaram, "Superconducting properties, electrical resistivities, and structure of NbN thin films," *J. Appl. Phys.*, vol. 44, no. 12, pp. 5539–5545, 1973.

[32] J. R. Clem and K. K. Berggren, "Geometry-dependent critical currents in superconducting nanocircuits," *Phys. Rev. B*, vol. 84, no. 17, p. 174510, Nov. 2011.

[33] F. Najafi, J. Mower, N. C. Harris, F. Bellei, A. Dane, C. Lee, X. Hu, P. Kharel, F. Marsili, S. Assefa, K. K. Berggren, and D. Englund, "On-chip detection of non-classical light by scalable integration of single-photon detectors.," *Nat. Commun.*, vol. 6, p. 5873, 2015.

[34] Y. Ivry, C.-S. Kim, A. E. Dane, D. De Fazio, A. N. McCaughan, K. a. Sunter, Q. Zhao, and K. K. Berggren, "Universal scaling of the critical temperature for thin films near the superconducting-to-insulating transition," *Phys. Rev. B*, vol. 90, no. 21, p. 214515, Dec. 2014.

[35] J. M. Shainline, S. M. Buckley, N. Nader, C. M. Gentry, K. C. Cossel, J. W. Cleary, M. Popović, N. R. Newbury, S. W. Nam, and R. P. Mirin, "Room-temperature-deposited dielectrics and superconductors for integrated photonics," *Opt. Express*, vol. 25, no. 9, p. 10322, 2017.

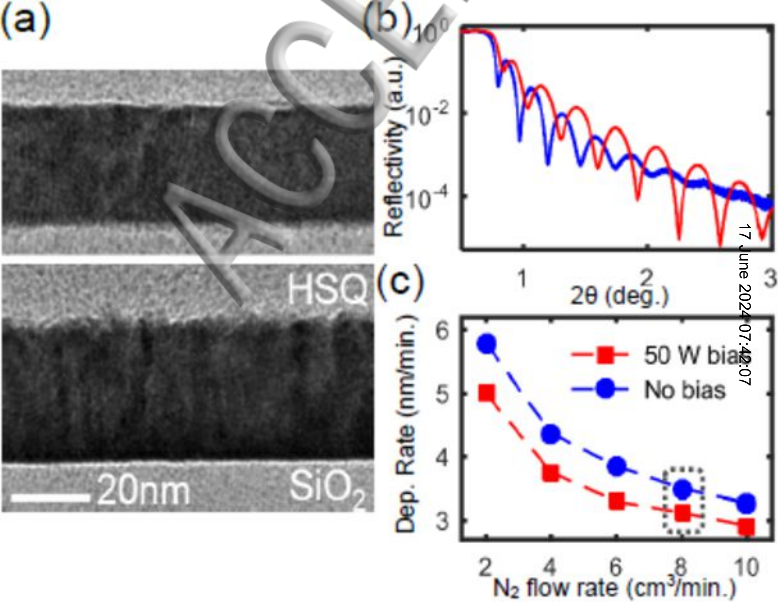
(a)
HSQ
SiO$_2$
20nm
(b)
10^0
10^{-2}
10^{-4}
Reflectivity (a.u.)
1
2
3
2θ (deg.)
(c)
6
5
4
3
Dep. Rate (nm/min.)
50 W bias
No bias
2
4
6
8
10
N$_2$ flow rate (cm^3/min.)

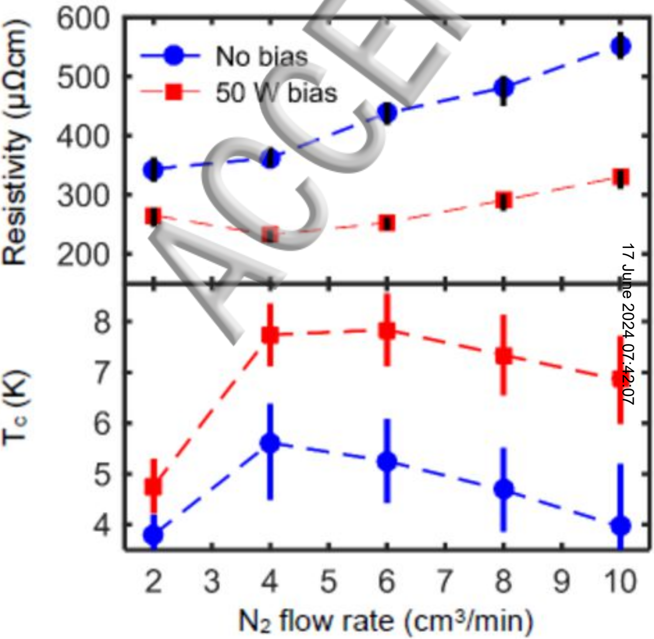
600
500
400
300
200
Resistivity (μΩcm)
No bias
50 W bias
8
7
6
5
4
T_C (K)
2
3
4
5
6
7
8
9
10
N₂ flow rate (cm³/min)

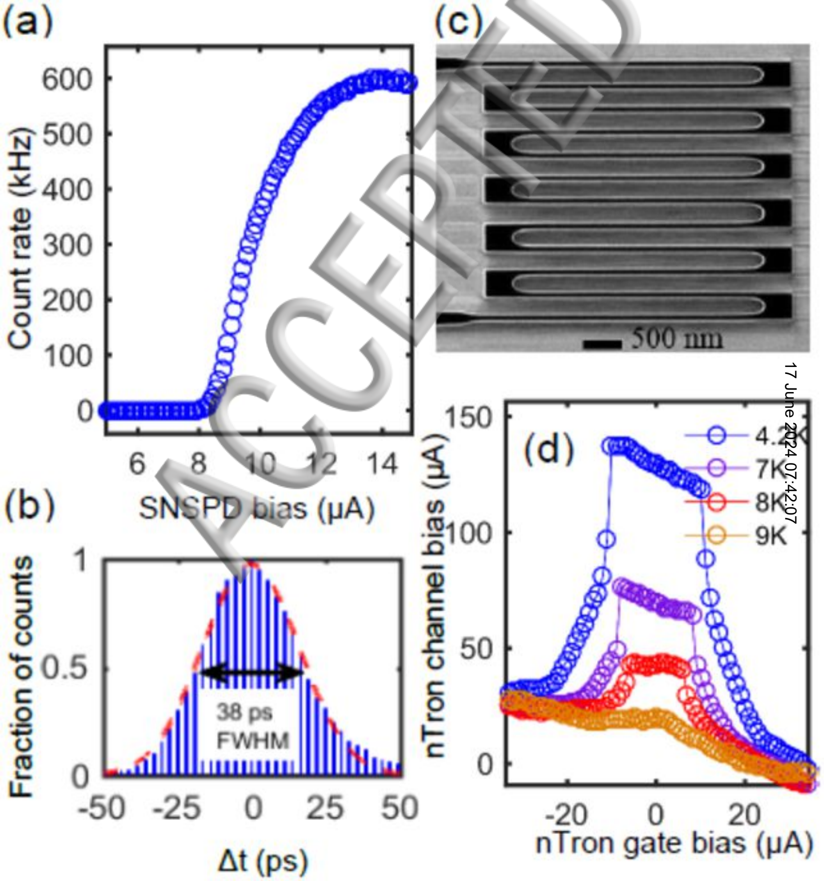
(a)
Count rate (kHz)
0
100
200
300
400
500
600
6
8
10
12
14
SNSPD bias (μA)
(b)
Fraction of counts
0
0.5
1
38 ps
FWHM
-50
-25
0
25
50
Δt (ps)
(c)
500 nm
(d)
nTron channel bias (μA)
0
50
100
150
4.2K
7K
8K
9K
-20
0
20
nTron gate bias (μA)